Density-dependent delta interactions and actinide pairing matrix elements*

R. R. Chasman
Chemistry Division, Argonne National Laboratory, Argonne, Illinois 60439
(Received 28 June 1976)

A density-dependent δ interaction is used to calculate pairing matrix elements for actinide proton and neutron orbitals. Tables of the matrix elements are given. The Seniority-one spectra of odd-mass actinides are analyzed in terms of these matrix elements. Several features of actinide spectra that cannot be understood with constant pairing matrix elements are explained with the density-dependent matrix elements.

[NUCLEAR STRUCTURE Density-dependent δ interaction; pairing matrix elements; actinides; calculated single particle levels; deduced deformations.]

I. INTRODUCTION

In this work, we use a density-dependent δ interaction (DDDI) to calculate pairing matrix elements for actinide proton and neutron orbitals. We infer reasonable values for the parameters of the DDDI by making use of experimental data on excitation energies in odd and even mass actinides.

Our motivations for a residual interaction of the density-dependent form are multiple. The primary motivation for this approach is the success of the surface δ interaction (SDI) in explaining many features of residual interaction matrix elements.[1,2] We regard the DDDI as a somewhat less schematic form of the SDI. Secondly, the work of Migdal[3,4] strongly motivates the use of a density-dependent residual interaction, with major contributions to the residual interaction coming from the nuclear surface region. A third motivation is provided by the success of a Skyrme force[5] in the nuclear Hartree-Fock calculations, particularly in the actinide[6] region. Here, a repulsive three-body force, which is equivalent in most respects to a density-dependent two-body interaction, is used to guarantee the saturation of nuclear forces. Another sort of motivation, which is basic for all forms of δ interactions, is the enormous calculational simplicity of δ interactions *vis a vis* interactions of finite range. Because of the difficulty of evaluating finite range matrix elements, the single particle wave functions used for such purposes must be severely truncated; usually they are restricted to a single oscillator shell basis set and are not a good representation of Woods-Saxon single particle eigenfunctions. With a δ interaction, it is a relatively simple and speedy matter to calculate two-body matrix elements using realistic Woods-Saxon single particle wave functions. This feature of δ interactions is important for the calculations we discuss here as they involve some 900 different two-body matrix elements.

In Sec. II, we discuss the parameters of the two-body interaction, how the parameters are determined, and give tables of pairing matrix elements for the 30 proton and 30 neutron orbitals that we have used in our calculations. We present the Hamiltonian considered in the calculations and some discussion of the proper terms to subtract from it. In Sec. III, we present the single particle spectra of odd mass actinides calculated using the DDDI matrix elements and compare these results with results obtained using constant pairing matrix elements. We also present the apparent nuclear deformations that emerge from this calculation when the DDDI single particle spectra are compared with single particle spectra of a momentum-dependent Woods-Saxon potential.[7]

II. DDDI AND HAMILTONIAN

The two-body interactions we consider here are of the form

$$V(\vec{r},\tilde{\rho}(\vec{r})) = -V_0\delta(\vec{r}_i-\vec{r}_j)\left[1-\left(\frac{\tilde{\rho}(\vec{r})}{B}\right)^{\eta}\right], \qquad (1)$$

where $\vec{r}$ denotes the two-body center of mass coordinate and $\tilde{\rho}(\vec{r})$ denotes a typical nuclear density at the point $\vec{r}$. We do not want to formulate an interaction in terms of actual densities $\rho(\vec{r})$ because that would involve a separate calculation of two-body matrix elements for every state in every nucleus. There are three parameters in this residual interaction—V_0, B, and η. For the two-body $T=1$ pairing matrix elements, the parameter V_0 subsumes contributions from two different terms, i.e.,

$$V_0 = V_1 + V_2\vec{\sigma}\cdot\vec{\sigma}, \qquad (2)$$

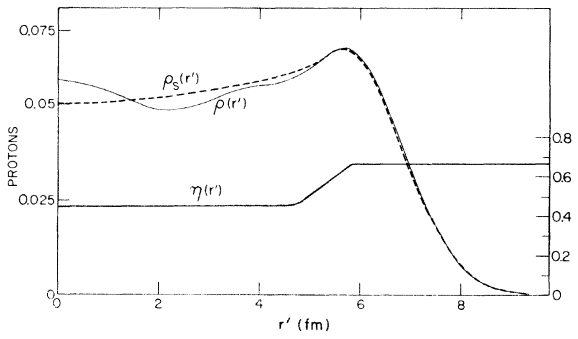

FIG. 1. Proton density for $Z = 96$. The solid curve is obtained by averaging over equipotential surfaces. The dashed curve is a smoothed density. The density scale is on the left. $\eta(r')$ and r' are defined in the text. The scale for $\eta(r')$ is on the right.

with the two terms having pairing matrix elements that are proportional to each other. In the limit $B \to \infty$, the interaction of Eq. (1) is a simple δ interaction. We have searched matrix element sets with $B \simeq \rho_0$, where ρ_0 is an interior nuclear density. With values of B in this range, most of the contribution to the matrix elements comes from the nuclear surface region. Our motivation here is the SDI. We should note, however, that the DDDI with $B \simeq \rho_0$ will not normally give matrix elements that are the same as the SDI. The SDI is idealized by assuming that all relevant orbitals have equal radial amplitudes in the region that the two-body interaction takes place. If we examine Woods-Saxon wave functions in the nuclear surface region and the exterior region by averaging the wave function intensities over equipotential surfaces, we find that the differences in these intensities are ~40%. This suggests the possibility of differences in the DDDI and SDI matrix elements. The third parameter is the exponent η. For neutrons, we have adopted the value of $\frac{2}{3}$ for η, as a dependence of the two-body interaction on this power of the density is expected on fundamental grounds.[8] We mention that one can get similar matrix elements with different choices of η, e.g., $\eta = 1$. For protons, we use a somewhat more complicated form for η, as will be discussed below.

The physical picture that we associate with this form of the residual interaction is a simple one. Because of saturation effects, the nuclear interior region is an energetically unfavorable region for nucleons to be and to interact. The interaction that we have described in Eq. (1) is consistent with this picture for neutrons. However, the situation for proton interactions is complicated by Coulomb repulsion effects. Because of Coulomb repulsion effects, the density of protons is reduced in the nuclear interior region. If we were to simply use the interaction of Eq. (1), the interaction probability for protons would be enhanced in the interior region. However, as this region is an energetically unfavored one for protons, this enhancement is spurious in our picture. We have corrected crudely for this effect by giving η a reduced value for protons in the nuclear interior region. Another way to correct for this feature would be to introduce another term into Eq. (1) proportional to the Coulomb field at point $\vec{r}$.

In the calculations we report here, we have used as our typical proton and neutron densities $\tilde{\rho}_P(\vec{r})$ and $\tilde{\rho}_N(\vec{r})$ the densities obtained from single particle wave functions calculated[7] for ^{244}Cm, with the deformations $\epsilon_2 = 0.24$ and $\epsilon_4 = 0.00$. The densities that we have used are the sums of the first 96 proton wave function densities and 148 neutron densities, respectively. These densities appear to be fairly typical of the actinides and ^{244}Cm is in the middle of the actinide region. The density distribution we get for $Z = 92$ is quite similar to that of Ref. 9. The matrix elements that we have calculated with these densities do not appear to be overly sensitive to the details of the density distribution. After completing the calculations reported here, we reevaluated the matrix elements using smoothed density distributions and obtained rather similar matrix element sets. In Fig. 1, we have plotted the density distribution of protons that we get for the first 96 protons. The densities are given as a function of r', where

$$r' = (\omega_\rho{}^2\rho^2 + \omega_z{}^2 Z^2)^{1/2} \tag{3}$$

and the values of the density have been averaged over the surfaces defined by different values of r'. We also display in Fig. 1 the value of $\eta(r')$ used in our calculations. Most of the proton orbitals seen extensively in the actinides do not have large interior amplitudes and their matrix elements are insensitive to $\eta(r')$. However, the proton orbital $\frac{3}{2}-[521]$ does have a peak in the interior region and we have used experimental data on this orbital to guide us in the matter of suppressing interior contributions to the proton matrix elements. Specifically, we have chosen the interior value of $\eta(r')$ to make the average pairing matrix element involving the orbital $\frac{3}{2}-[521]$ slightly weaker than the average pairing matrix element involving the orbital $\frac{7}{2}+[633]$ as indicated by the experimental data.

Quite generally, our criterion for determining the parameters of the DDDI is that the pairing matrix elements obtained from the DDDI explain the known excitation energies of the seniority-

one levels in the actinides in as reasonable a manner as possible. By reasonable, we mean that the changes in single particle energy from one nucleus to its neighbor should be consistent with small changes in the deformation parameters. This criterion is useful in establishing the relative magnitudes of the matrix elements associated with the actinide orbitals. However, it is not too useful for determining the overall strength of the interaction as the calculated excitation energies of seniority-one states are somewhat insensitive to the overall strength. The excitation energies of the seniority-two states in the even actinides are quite sensitive to the overall strength of the interaction and we have utilized data on high spin seniority-two states to determine the overall strength. We specify high spin states ($I > 2$) as these are least likely to be shifted in energy by configuration interaction effects. These criteria do not determine a unique set of parameters for the DDDI, as many different parameter choices give similar sets of matrix elements.

For neutron orbitals, the potential that we use is

$$V_N(\vec{r}, \tilde{\rho}_N(\vec{r})) = -23.66\ \text{MeV}\ \delta(\vec{r}_i - \vec{r}_j) \times \left[1 - \left(\frac{\tilde{\rho}_N(\vec{r})}{0.077}\right)^{2/3}\right], \quad (4)$$

where $\tilde{\rho}_N(\vec{r})$ is the neutron density in ^{244}Cm discussed above and has a value of 0.072 in the nuclear interior. The details of $\tilde{\rho}_N(\vec{r})$ depend strongly on the parameters of the one-body potential. Other choices of the single particle potential parameters will give rise to different densities and hence different choices of V_0 and B. The essential feature here is that B is slightly larger than the interior neutron density.

In Table I, we have tabulated the neutron pairing matrix elements of the actinide orbitals used in our calculations. The orbitals are identified in terms of the asymptotic quantum numbers in Table III. There are some rather interesting features in these matrix elements:

1. There is an enhancement of matrix elements for pairs of orbitals with similar values of the asymptotic n_z quantum number which we denote the prolate-oblate effect. This effect can be seen most easily be constructing the matrix element ratios

$$R_{i,j} = V_{i,j}/[V_{i,i} \times V_{j,j}]^{1/2}. \quad (5)$$

This same effect has been noted[10] for SDI matrix elements.

2. There is a large radial effect that is seen in the magnitudes of diagonal matrix elements $V_{i,i}$. This effect is particularly noticeable for the $j_{15/2}$ orbitals seen in the actinides such as $\frac{5}{2}-[752]$, $\frac{7}{2}-[743]$, and $\frac{9}{2}-[734]$ and the $i_{13/2}$ orbital $\frac{13}{2}+[606]$. For these orbitals, the diagonal matrix elements are 0.28, 0.28, 0.29, and 0.40 MeV, respectively, while the average diagonal matrix element for neutron orbitals is 0.23 MeV. Most of the orbitals with very large diagonal matrix elements are far from the Fermi level throughout the actinide region. Orbitals such as the $\frac{1}{2}+[631]$, $\frac{5}{2}+[622]$, $\frac{3}{2}+[622]$, and $\frac{7}{2}+[624]$ have much smaller diagonal matrix elements (~0.15 MeV on the average). The reason for this effect is that the major radial peaks of the $j_{15/2}$ wave functions extend further into the low density region than do the other wave functions. There is a second radial effect.

3. Orbitals with external radial peaks near each other have relatively enhanced matrix elements. This can be seen in the matrix element for the orbitals $\frac{1}{2}+[631]$ and $\frac{1}{2}-[501]$. For this matrix element, the quantity $R_{i,j}$ has the value of 0.35. For the pairing matrix element of the orbitals $\frac{1}{2}-[501]$ and $\frac{7}{2}+[624]$, $R_{i,j}$ has the value 0.26. Rather crudely, we might characterize the matrix elements as

$$V_{i,j} \approx [V_{i,i} \times V_{j,j}]^{1/2} \exp[-\alpha(\theta_i - \theta_j)^2] \times \exp[-\beta(\langle N_i - l_i\rangle - \langle N_j - l_j\rangle)^2], \quad (6)$$

where α and β are numerical constants and θ_i, $\langle N_i\rangle$, and $\langle l_i\rangle$ are expectation values of single particle wave functions

$$\theta_i^{\,2} = \cos^{-1}(\langle N_{z_i}\rangle / \langle N_i\rangle), \quad (7a)$$

$$\langle N_i\rangle = \langle N_{z_i} + N_{\perp i}\rangle. \quad (7b)$$

Each of the terms in Eq. (6) is meant to account for one of the features that we have noted above.

For the proton orbitals, the potential we use is

$$V_P(\vec{r}, \rho_P(\vec{r})) = -20.06\ \text{MeV}\ \delta(\vec{r}_i - \vec{r}_j) \times \left[1 - \left(\frac{\tilde{\rho}_P(\vec{r})}{0.0737}\right)^{\eta(\vec{r})}\right], \quad (8)$$

where $\eta(\vec{r})$ is easily determined from $\eta(r')$ shown in Fig. 1. The pairing matrix elements for the actinide proton orbitals are given in Table II and the orbital numbers are identified in Table III. There are the same sorts of angular and radial correlations for the proton matrix elements that we have noted for the neutron matrix elements. Matrix elements involving the $i_{13/2}$ proton orbitals such as $\frac{5}{2}+[642]$ and $\frac{7}{2}+[633]$ are somewhat larger than average. Matrix elements involving the $h_{9/2}$ orbitals such as $\frac{5}{2}-[523]$ are somewhat smaller than average. This latter feature occurs because the radial peak in the $h_{9/2}$ orbital is buried

TABLE I. Neutron pairing matrix elements obtained with the DDDI. All matrix elements are in MeV and should be multiplied by −1.

	1	2	3	4	5	6	7	8	9	10	11	12	13	14	15	16	17	18	19	20	21	22	23	24	25	26	27	28	29	30
1	0.31	0.13	0.07	0.05	0.12	0.06	0.05	0.07	0.04	0.05	0.04	0.04	0.03	0.04	0.03	0.05	0.32	0.03	0.23	0.04	0.25	0.03	0.12	0.03	0.15	0.03	0.07	0.06	0.05	0.04
2	0.13	0.18	0.11	0.08	0.14	0.09	0.07	0.09	0.06	0.06	0.05	0.05	0.03	0.06	0.05	0.06	0.14	0.05	0.15	0.06	0.16	0.05	0.13	0.04	0.17	0.04	0.14	0.08	0.07	0.06
3	0.07	0.11	0.14	0.11	0.09	0.12	0.08	0.10	0.07	0.07	0.05	0.05	0.04	0.06	0.05	0.10	0.09	0.06	0.11	0.07	0.10	0.06	0.10	0.04	0.11	0.04	0.13	0.13	0.07	0.06
4	0.05	0.08	0.11	0.22	0.05	0.09	0.12	0.07	0.12	0.09	0.08	0.06	0.05	0.08	0.06	0.16	0.06	0.08	0.09	0.10	0.06	0.08	0.07	0.06	0.07	0.06	0.08	0.11	0.13	0.08
5	0.12	0.14	0.09	0.05	0.17	0.09	0.06	0.11	0.06	0.07	0.05	0.06	0.04	0.07	0.05	0.05	0.15	0.03	0.09	0.05	0.18	0.03	0.12	0.04	0.20	0.04	0.17	0.09	0.08	0.06
6	0.06	0.09	0.12	0.09	0.09	0.13	0.09	0.12	0.09	0.08	0.06	0.06	0.05	0.08	0.06	0.07	0.08	0.05	0.07	0.08	0.10	0.05	0.09	0.06	0.11	0.06	0.14	0.15	0.09	0.07
7	0.05	0.07	0.08	0.12	0.06	0.09	0.13	0.08	0.13	0.10	0.09	0.07	0.05	0.09	0.07	0.10	0.06	0.07	0.06	0.11	0.06	0.07	0.07	0.07	0.08	0.07	0.09	0.12	0.14	0.08
8	0.07	0.09	0.10	0.07	0.11	0.12	0.08	0.16	0.08	0.12	0.06	0.08	0.04	0.09	0.07	0.06	0.11	0.04	0.05	0.07	0.12	0.04	0.08	0.05	0.15	0.05	0.18	0.19	0.11	0.09
9	0.04	0.06	0.07	0.12	0.06	0.09	0.13	0.08	0.14	0.12	0.10	0.08	0.07	0.11	0.08	0.10	0.06	0.06	0.05	0.11	0.07	0.06	0.07	0.08	0.08	0.08	0.10	0.13	0.16	0.10
10	0.05	0.06	0.07	0.09	0.07	0.08	0.10	0.12	0.12	0.18	0.09	0.12	0.06	0.15	0.10	0.09	0.09	0.05	0.03	0.10	0.10	0.05	0.05	0.06	0.11	0.06	0.13	0.18	0.22	0.13
11	0.04	0.05	0.05	0.08	0.05	0.06	0.09	0.06	0.10	0.09	0.16	0.12	0.10	0.16	0.11	0.14	0.05	0.09	0.04	0.15	0.06	0.09	0.06	0.11	0.06	0.11	0.07	0.09	0.12	0.17
12	0.04	0.05	0.05	0.06	0.06	0.06	0.07	0.08	0.08	0.12	0.12	0.19	0.08	0.24	0.15	0.11	0.08	0.07	0.03	0.12	0.08	0.07	0.04	0.09	0.09	0.09	0.11	0.13	0.18	0.24
13	0.03	0.03	0.04	0.05	0.04	0.05	0.05	0.04	0.07	0.06	0.10	0.08	0.18	0.11	0.19	0.07	0.04	0.15	0.03	0.08	0.04	0.15	0.04	0.17	0.05	0.19	0.05	0.06	0.08	0.11
14	0.04	0.06	0.06	0.08	0.07	0.08	0.09	0.09	0.11	0.15	0.16	0.24	0.11	0.32	0.21	0.15	0.10	0.10	0.04	0.17	0.10	0.10	0.05	0.12	0.12	0.12	0.14	0.17	0.23	0.33
15	0.03	0.05	0.05	0.06	0.05	0.06	0.07	0.07	0.08	0.10	0.11	0.15	0.19	0.21	0.40	0.09	0.08	0.17	0.03	0.10	0.09	0.17	0.04	0.21	0.10	0.22	0.11	0.13	0.16	0.23
16	0.05	0.06	0.10	0.16	0.05	0.07	0.10	0.06	0.10	0.09	0.14	0.11	0.07	0.15	0.09	0.23	0.05	0.11	0.08	0.14	0.06	0.10	0.06	0.09	0.06	0.09	0.08	0.10	0.13	0.15
17	0.32	0.14	0.09	0.06	0.15	0.08	0.06	0.11	0.06	0.09	0.05	0.08	0.04	0.10	0.08	0.05	0.43	0.04	0.23	0.06	0.28	0.04	0.11	0.04	0.19	0.04	0.15	0.12	0.11	0.09
18	0.03	0.05	0.06	0.08	0.03	0.05	0.07	0.04	0.06	0.05	0.09	0.07	0.15	0.10	0.17	0.11	0.04	0.21	0.05	0.08	0.04	0.21	0.04	0.15	0.04	0.16	0.05	0.06	0.08	0.11
19	0.23	0.15	0.11	0.09	0.09	0.07	0.06	0.05	0.05	0.03	0.04	0.03	0.03	0.04	0.03	0.08	0.23	0.05	0.31	0.06	0.18	0.05	0.12	0.04	0.10	0.03	0.06	0.05	0.04	0.04
20	0.04	0.06	0.07	0.10	0.05	0.08	0.11	0.07	0.11	0.10	0.15	0.12	0.08	0.17	0.10	0.14	0.06	0.08	0.06	0.17	0.06	0.09	0.07	0.10	0.07	0.10	0.09	0.11	0.15	0.17
21	0.25	0.16	0.10	0.06	0.18	0.10	0.06	0.12	0.07	0.10	0.06	0.08	0.04	0.10	0.09	0.06	0.28	0.04	0.18	0.06	0.32	0.04	0.13	0.05	0.23	0.05	0.16	0.14	0.12	0.10
22	0.03	0.05	0.06	0.08	0.03	0.05	0.07	0.04	0.06	0.05	0.09	0.07	0.15	0.10	0.17	0.10	0.04	0.21	0.05	0.09	0.04	0.21	0.04	0.15	0.04	0.16	0.05	0.06	0.08	0.11
23	0.12	0.13	0.10	0.07	0.12	0.09	0.07	0.08	0.07	0.05	0.06	0.04	0.04	0.05	0.04	0.06	0.11	0.04	0.12	0.07	0.13	0.04	0.14	0.05	0.14	0.05	0.11	0.07	0.06	0.05
24	0.03	0.04	0.04	0.06	0.04	0.06	0.07	0.05	0.08	0.06	0.11	0.09	0.17	0.12	0.21	0.09	0.04	0.15	0.04	0.10	0.05	0.15	0.05	0.19	0.05	0.19	0.06	0.07	0.09	0.13
25	0.15	0.17	0.11	0.07	0.20	0.11	0.08	0.15	0.08	0.11	0.06	0.09	0.05	0.12	0.10	0.06	0.19	0.04	0.10	0.07	0.23	0.04	0.14	0.05	0.28	0.05	0.21	0.16	0.14	0.11
26	0.03	0.04	0.04	0.06	0.04	0.06	0.07	0.05	0.08	0.06	0.11	0.09	0.19	0.12	0.22	0.09	0.04	0.16	0.03	0.10	0.05	0.16	0.05	0.19	0.05	0.20	0.06	0.07	0.09	0.13
27	0.07	0.14	0.13	0.08	0.17	0.14	0.09	0.18	0.10	0.13	0.07	0.11	0.05	0.14	0.11	0.08	0.15	0.05	0.06	0.09	0.16	0.05	0.11	0.06	0.21	0.06	0.28	0.21	0.16	0.13
28	0.06	0.08	0.13	0.11	0.09	0.15	0.12	0.19	0.13	0.18	0.09	0.13	0.06	0.17	0.13	0.10	0.12	0.06	0.05	0.11	0.14	0.06	0.07	0.07	0.16	0.07	0.21	0.29	0.22	0.16
29	0.05	0.07	0.07	0.13	0.08	0.09	0.14	0.11	0.16	0.22	0.12	0.18	0.08	0.23	0.16	0.13	0.11	0.08	0.04	0.15	0.12	0.08	0.06	0.09	0.14	0.09	0.16	0.22	0.32	0.22
30	0.04	0.06	0.06	0.08	0.06	0.07	0.08	0.09	0.10	0.13	0.17	0.24	0.11	0.33	0.23	0.15	0.09	0.11	0.04	0.17	0.10	0.11	0.05	0.13	0.11	0.13	0.13	0.16	0.22	0.34

TABLE II. Proton pairing matrix elements obtained with the DDDI. All matrix elements are in MeV and should be multiplied by −1.

	1	2	3	4	5	6	7	8	9	10	11	12	13	14	15	16	17	18	19	20	21	22	23	24	25	26	27	28	29	30
1	0.36	0.06	0.25	0.16	0.06	0.24	0.15	0.06	0.18	0.15	0.13	0.11	0.10	0.26	0.14	0.10	0.37	0.06	0.15	0.09	0.28	0.07	0.12	0.08	0.19	0.10	0.06	0.11	0.09	0.10
2	0.06	0.44	0.09	0.08	0.22	0.06	0.07	0.23	0.06	0.07	0.09	0.12	0.19	0.07	0.12	0.13	0.05	0.26	0.06	0.10	0.05	0.13	0.07	0.14	0.06	0.09	0.24	0.11	0.14	0.18
3	0.25	0.09	0.33	0.17	0.09	0.19	0.13	0.09	0.10	0.07	0.06	0.05	0.04	0.22	0.22	0.16	0.25	0.13	0.11	0.14	0.21	0.12	0.07	0.10	0.13	0.06	0.08	0.05	0.04	0.04
4	0.16	0.08	0.17	0.25	0.09	0.17	0.18	0.09	0.16	0.10	0.08	0.07	0.06	0.17	0.22	0.16	0.16	0.10	0.14	0.14	0.16	0.12	0.09	0.11	0.16	0.07	0.09	0.07	0.06	0.06
5	0.06	0.22	0.09	0.09	0.32	0.06	0.09	0.32	0.07	0.08	0.10	0.13	0.21	0.07	0.10	0.12	0.06	0.13	0.07	0.14	0.06	0.19	0.08	0.19	0.06	0.10	0.29	0.12	0.16	0.21
6	0.24	0.06	0.19	0.17	0.06	0.29	0.18	0.07	0.22	0.16	0.14	0.12	0.10	0.23	0.15	0.10	0.24	0.07	0.17	0.10	0.29	0.08	0.13	0.08	0.26	0.11	0.06	0.13	0.09	0.10
7	0.15	0.07	0.13	0.18	0.09	0.18	0.21	0.09	0.19	0.12	0.09	0.07	0.06	0.17	0.16	0.15	0.15	0.09	0.16	0.15	0.17	0.12	0.11	0.12	0.19	0.08	0.09	0.08	0.06	0.06
8	0.06	0.23	0.09	0.09	0.32	0.07	0.09	0.32	0.07	0.08	0.10	0.14	0.21	0.07	0.09	0.11	0.06	0.13	0.07	0.14	0.06	0.19	0.08	0.19	0.07	0.10	0.31	0.13	0.16	0.21
9	0.18	0.06	0.10	0.16	0.07	0.22	0.19	0.07	0.28	0.21	0.16	0.14	0.12	0.16	0.15	0.12	0.18	0.07	0.20	0.12	0.21	0.08	0.15	0.08	0.26	0.12	0.07	0.14	0.10	0.12
10	0.15	0.07	0.07	0.10	0.08	0.16	0.12	0.08	0.21	0.29	0.21	0.16	0.14	0.09	0.14	0.14	0.16	0.09	0.20	0.14	0.17	0.10	0.20	0.10	0.19	0.14	0.07	0.17	0.12	0.14
11	0.13	0.09	0.06	0.08	0.10	0.14	0.09	0.10	0.16	0.21	0.31	0.22	0.16	0.09	0.07	0.14	0.13	0.11	0.11	0.15	0.14	0.12	0.23	0.13	0.16	0.19	0.09	0.23	0.14	0.17
12	0.11	0.12	0.05	0.07	0.13	0.12	0.07	0.14	0.14	0.16	0.22	0.34	0.22	0.07	0.07	0.08	0.11	0.14	0.10	0.09	0.12	0.16	0.14	0.17	0.13	0.26	0.12	0.33	0.19	0.23
13	0.10	0.19	0.04	0.06	0.21	0.10	0.06	0.21	0.12	0.14	0.16	0.22	0.41	0.06	0.06	0.07	0.10	0.08	0.08	0.08	0.10	0.09	0.11	0.10	0.11	0.16	0.21	0.20	0.32	0.40
14	0.26	0.07	0.22	0.17	0.07	0.23	0.17	0.07	0.16	0.09	0.09	0.07	0.06	0.25	0.15	0.11	0.27	0.08	0.14	0.11	0.24	0.09	0.10	0.08	0.19	0.08	0.07	0.07	0.06	0.06
15	0.14	0.12	0.22	0.22	0.10	0.15	0.16	0.09	0.15	0.14	0.07	0.07	0.06	0.15	0.34	0.22	0.14	0.15	0.14	0.18	0.14	0.12	0.08	0.11	0.15	0.06	0.07	0.07	0.05	0.06
16	0.10	0.13	0.16	0.16	0.12	0.10	0.15	0.11	0.12	0.14	0.14	0.08	0.07	0.11	0.22	0.30	0.09	0.18	0.11	0.28	0.10	0.18	0.12	0.15	0.11	0.07	0.09	0.09	0.05	0.07
17	0.37	0.05	0.25	0.16	0.06	0.24	0.15	0.06	0.18	0.16	0.13	0.11	0.10	0.27	0.14	0.09	0.38	0.06	0.15	0.09	0.27	0.07	0.12	0.07	0.20	0.10	0.06	0.12	0.09	0.10
18	0.06	0.26	0.13	0.10	0.13	0.07	0.09	0.13	0.07	0.09	0.11	0.14	0.08	0.08	0.15	0.18	0.06	0.45	0.07	0.14	0.06	0.19	0.09	0.19	0.07	0.11	0.12	0.14	0.07	0.08
19	0.15	0.06	0.11	0.14	0.07	0.17	0.16	0.07	0.20	0.20	0.11	0.10	0.08	0.14	0.14	0.11	0.15	0.07	0.20	0.12	0.17	0.09	0.14	0.09	0.19	0.11	0.08	0.10	0.09	0.08
20	0.09	0.10	0.14	0.14	0.14	0.10	0.15	0.14	0.12	0.14	0.15	0.09	0.08	0.11	0.18	0.28	0.09	0.14	0.12	0.29	0.10	0.20	0.13	0.18	0.11	0.08	0.11	0.10	0.06	0.08
21	0.28	0.05	0.21	0.16	0.06	0.29	0.17	0.06	0.21	0.17	0.14	0.12	0.10	0.24	0.14	0.10	0.27	0.06	0.17	0.10	0.31	0.07	0.13	0.08	0.23	0.11	0.06	0.12	0.09	0.10
22	0.07	0.13	0.12	0.12	0.19	0.08	0.12	0.19	0.08	0.10	0.12	0.16	0.09	0.09	0.12	0.18	0.07	0.19	0.09	0.20	0.07	0.29	0.10	0.28	0.08	0.13	0.16	0.16	0.08	0.10
23	0.12	0.07	0.07	0.09	0.08	0.13	0.11	0.08	0.15	0.20	0.23	0.14	0.11	0.10	0.08	0.12	0.12	0.09	0.14	0.13	0.13	0.10	0.21	0.11	0.14	0.15	0.08	0.15	0.11	0.11
24	0.08	0.14	0.10	0.11	0.19	0.08	0.12	0.19	0.08	0.10	0.13	0.17	0.10	0.08	0.11	0.15	0.07	0.19	0.09	0.18	0.08	0.28	0.11	0.29	0.08	0.14	0.18	0.17	0.09	0.11
25	0.19	0.06	0.13	0.16	0.06	0.26	0.19	0.07	0.26	0.19	0.16	0.13	0.11	0.19	0.15	0.11	0.20	0.07	0.19	0.11	0.23	0.08	0.14	0.08	0.29	0.12	0.06	0.13	0.10	0.11
26	0.10	0.09	0.06	0.07	0.10	0.11	0.08	0.10	0.12	0.14	0.19	0.26	0.16	0.08	0.06	0.07	0.10	0.11	0.11	0.08	0.11	0.13	0.15	0.14	0.12	0.23	0.10	0.25	0.16	0.16
27	0.06	0.24	0.08	0.09	0.29	0.06	0.09	0.31	0.07	0.07	0.09	0.12	0.21	0.07	0.07	0.09	0.06	0.12	0.08	0.11	0.06	0.16	0.08	0.18	0.06	0.10	0.33	0.11	0.17	0.20
28	0.11	0.11	0.05	0.07	0.12	0.13	0.08	0.13	0.14	0.17	0.23	0.33	0.20	0.07	0.07	0.09	0.12	0.14	0.10	0.10	0.12	0.16	0.15	0.17	0.13	0.25	0.11	0.32	0.17	0.21
29	0.09	0.14	0.04	0.06	0.16	0.09	0.06	0.16	0.10	0.12	0.14	0.19	0.32	0.06	0.05	0.05	0.09	0.07	0.09	0.06	0.09	0.08	0.11	0.09	0.10	0.16	0.17	0.17	0.29	0.31
30	0.10	0.18	0.04	0.06	0.21	0.10	0.06	0.21	0.12	0.14	0.17	0.23	0.40	0.06	0.06	0.07	0.10	0.08	0.08	0.08	0.10	0.10	0.11	0.11	0.11	0.16	0.20	0.21	0.31	0.40

TABLE III. Key to orbitals.

	Neutron orbitals	Proton orbitals
1	$\frac{1}{2}^+[651]$	$\frac{1}{2}^+[660]$
2	$\frac{1}{2}^+[640]$	$\frac{1}{2}^+[400]$
3	$\frac{1}{2}^+[631]$	$\frac{1}{2}^+[651]$
4	$\frac{1}{2}^+[620]$	$\frac{1}{2}^+[640]$
5	$\frac{3}{2}^+[642]$	$\frac{3}{2}^+[402]$
6	$\frac{3}{2}^+[631]$	$\frac{3}{2}^+[651]$
7	$\frac{3}{2}^+[622]$	$\frac{3}{2}^+[642]$
8	$\frac{5}{2}^+[633]$	$\frac{5}{2}^+[402]$
9	$\frac{5}{2}^+[622]$	$\frac{5}{2}^+[642]$
10	$\frac{7}{2}^+[624]$	$\frac{7}{2}^+[633]$
11	$\frac{7}{2}^+[613]$	$\frac{9}{2}^+[624]$
12	$\frac{9}{2}^+[615]$	$\frac{11}{2}^+[615]$
13	$\frac{9}{2}^+[604]$	$\frac{13}{2}^+[606]$
14	$\frac{11}{2}^+[615]$	$\frac{1}{2}^-[541]$
15	$\frac{13}{2}^+[606]$	$\frac{1}{2}^-[530]$
16	$\frac{1}{2}^-[510]$	$\frac{1}{2}^-[521]$
17	$\frac{1}{2}^-[770]$	$\frac{1}{2}^-[770]$
18	$\frac{1}{2}^-[501]$	$\frac{1}{2}^-[510]$
19	$\frac{1}{2}^-[750]$	$\frac{3}{2}^-[532]$
20	$\frac{3}{2}^-[512]$	$\frac{3}{2}^-[521]$
21	$\frac{3}{2}^-[761]$	$\frac{3}{2}^-[761]$
22	$\frac{3}{2}^-[501]$	$\frac{3}{2}^-[512]$
23	$\frac{3}{2}^-[752]$	$\frac{5}{2}^-[523]$
24	$\frac{5}{2}^-[503]$	$\frac{5}{2}^-[512]$
25	$\frac{5}{2}^-[752]$	$\frac{5}{2}^-[752]$
26	$\frac{7}{2}^-[503]$	$\frac{7}{2}^-[514]$
27	$\frac{7}{2}^-[743]$	$\frac{7}{2}^-[503]$
28	$\frac{9}{2}^-[734]$	$\frac{9}{2}^-[514]$
29	$\frac{11}{2}^-[725]$	$\frac{9}{2}^-[505]$
30	$\frac{13}{2}^-[716]$	$\frac{11}{2}^-[505]$

under the peak in the proton density distribution at $r' \simeq 5.8$ fm. A smaller value of B would give this orbital unrealistically small matrix elements.

The Hamiltonian that we have used in this study is

$$H = \sum_K \epsilon_K N_K - \sum_{\substack{i,j>0 \\ i\neq j}} V_{i,j} a_i^\dagger a_{-i}^\dagger a_{-j} a_j - \frac{1}{2}\sum_{i,j} W_{i,j} N_i N_j , \tag{9}$$

where ϵ_K denotes a single particle energy; N_K, a number operator; $a_i^\dagger(a_i)$, a fermion creation (annihilation) operator; and the index $-i$, the orbital that is the time reversal partner of orbital i. The quantities $V_{i,j}$ and $W_{i,j}$ are antisymmetrized matrix elements and are simply related to each other as

$$V_{i,j} = W_{i,j} + W_{i,-j}, \quad j \neq i, -i \tag{10a}$$

and

$$V_{i,i} \equiv W_{i,-i} . \tag{10b}$$

We have chosen to include the diagonal pairing matrix elements with the W matrix elements in Eq. (9) to emphasize that a part of their contribution to the total energy is already included in the single particle energies as is the case for the other matrix elements $W_{i,j}$. Specifically, we note that in the ground state of an even system

$$\sum_{i,j} W_{i,j} N_i N_j = \int d^3r \left(\sum_{i>0} \psi_i^2(\vec{r}) N_i\right) V(\vec{r}, \tilde{\rho}(\vec{r})) \times \left(\sum_{j>0} \psi_j^2(\vec{r}) N_j\right), \tag{11}$$

where $V(r, \tilde{\rho}(\vec{r}))$ is given by either Eq. (4) or (8) and $\psi_i^2(\vec{r})$ has already been summed over spin indices. From a Hartree-Fock point of view, we should subtract $\frac{1}{2}\langle \rho(\vec{r})\rangle$ from each of the wave function sums in Eq. (11) where the angled brackets around $\rho(\vec{r})$ denote a ground state expectation value. However, we are interested in the eigenvalues of a single particle potential that varies smoothly as a function of macroscopic parameters such as N (neutron number), Z, ϵ_2, and ϵ_4. Accordingly, we should subtract out only a smoothly varying part of the density in Eq. (11). We denote this smooth density as $\rho_S(\vec{r})$. Making this subtraction, we calculate the contributions to the energy from the terms $W'_{i,j}$ with

$$\sum_{i,j} W'_{i,j} N_i N_j = \int d^3r \left[\sum_{i>0} \psi_i^2(\vec{r}) N_i - \tfrac{1}{2}\rho_S(\vec{r})\right] \times V(\vec{r}, \tilde{\rho}(\vec{r})) \left[\sum_{j>0} \psi_j^2(\vec{r}) N_j - \tfrac{1}{2}\rho_S(\vec{r})\right] . \tag{12}$$

We must at the same time realize that our single particle energies are obtained from a potential that includes $\rho_S(\vec{r}) V(\vec{r}, \tilde{\rho}(\vec{r}))$. We assume here that the contribution from this term is accommodated by the choice of parameters that one makes in defining the Woods-Saxon potential. If we were to formulate the two-body interaction in terms of the actual density for each configuration, this would entail the inclusion of an extra term D in the evaluation of the energy for each configuration with

$$D = \int d^3r \left(\sum_{i>0} \psi_i^2(\vec{r}) N_i \right) \rho_S(\vec{r}) [\, V(\vec{r}, \rho(\vec{r})) - V(\vec{r}, \rho_S(\vec{r}))] . \tag{13}$$

The effect of residual interactions is to smooth out the true density distribution and hopefully the contributions from this term would be small. For seniority-one and seniority-two states, Eq. (12) must be modified slightly; we have taken those changes into account in our calculations.

The smoothed density distribution that we use is constructed in two stages. First the density is averaged over surfaces defined by values of r' at intervals of $0.05R_0$. This is the density distribution displayed in Fig. 1, and a similar distribution was calculated for many values of Z and N. The resulting density distributions were then fitted by smooth functions whose parameters vary linearly as functions of N and Z. For neutrons, the smoothed density distribution we use is of the form

$$\rho_S(r) = A_0, \quad 0 < r' < r_1, \tag{14a}$$

$$\rho_S(r') = A_1 / \{1 + \exp[(r' - R_1)/a_1]\}, \quad r' > r_1, \tag{14b}$$

where the parameters A_0, A_1, R_1, a_1, and r_1 have linear dependence on N and the variable r' is defined in Eq. (3). The linear dependence on N is needed to compensate for the fact that all densities were calculated with the ^{244}Cm wave functions.

The smoothed proton density that we use is

$$\rho_S(r') = A_0 + A_1(r')^2, \quad 0 < r' < r_1, \tag{15a}$$

$$\rho_S(r') = A_2 \{\exp - [(r' - R_2)/a_2]^2\}, \quad r_1 < r' < r_2, \tag{15b}$$

and

$$\rho_S(r') = A_3 / \{1 + \exp[(r' - R_3)/a_3]\}, \quad r' > r_2, \tag{15c}$$

where the parameters in Eq. (15) are linear functions of Z. We have included the smoothed density for $Z = 96$ in Fig. 1; it is given by the dashed line. The structure of the smoothed proton density is complicated relative to the neutron density because of Coulomb effects. The peak in the smoothed density at $r' \sim 5.8$ fm is just the reflection of a minimum in the proton single particle potential. For both proton and neutrons, most of the contribution to the matrix elements comes from the surface region. In this region the true density and the smoothed density are quite similar.

With all of the matrix elements in hand, the energies of the seniority-one states are calculated using the method of correlated quasi-particles.[11] A separate calculation is carried out for each state, blocking the appropriate level in each instance. The procedure is to assume a set of input single particle energies, ϵ_K, and with them calculate the energies of the seniority-one states. The single particle energies are then adjusted to bring the calculated energies into agreement with experimental observations. The single particle energies determined in this way will be referred to as extracted single particle energies. Having determined the extracted single particle energies, we calculate the excitation energies of seniority-two states in neighboring even isotopes. These energies are brought into overall agreement with experiment by adjusting V_0. The extracted single particle spectrum is then recalculated. Fortunately, the single particle level spacings are relatively insensitive to V_0 and this iteration procedure is possible.

Before examining the results of the calculations, it is worthwhile to point out the signatures of orbitals with pairing matrix elements that deviate substantially from the average values. Seniority-one states in which the blocked orbital has stronger then average matrix elements will appear at higher excitation energy than those involving blocked orbitals at the same single particle energy but having average matrix elements. For configurations having a blocked level with weaker than average matrix elements, the converse is true. These effects are particularly apparent when the orbital of interest is slightly below the Fermi level. In nuclei, these effects may be obscured by shifts in the single particle levels due to changes in the nuclear deformation or particle-vibration couplings.

We emphasize that the extracted single particle energies that we calculate are meaningful only in the context of the residual interaction that we consider. It would be incorrect to use these single particle energies with different pairing matrix elements, e.g., constant matrix elements.

III. RESULTS

For this analysis, we have taken data compiled for a forthcoming review article[12] on single particle states in the actinides. For our study of the neutron matrix elements, we consider levels in ^{233}U, ^{235}U, ^{237}U, ^{241}Pu, ^{245}Cm, ^{247}Cm, and the two 153 neutron isotones ^{249}Cm and ^{251}Cf. For the study of the proton matrix elements, we consider levels in ^{231}Pa, ^{237}Np, ^{241}Am, ^{243}Am, ^{249}Bk, and ^{251}Es. In Figs. 2 and 3, we have plotted the experimentally observed excitation energies of the seniority-one configurations, distinguishing be-

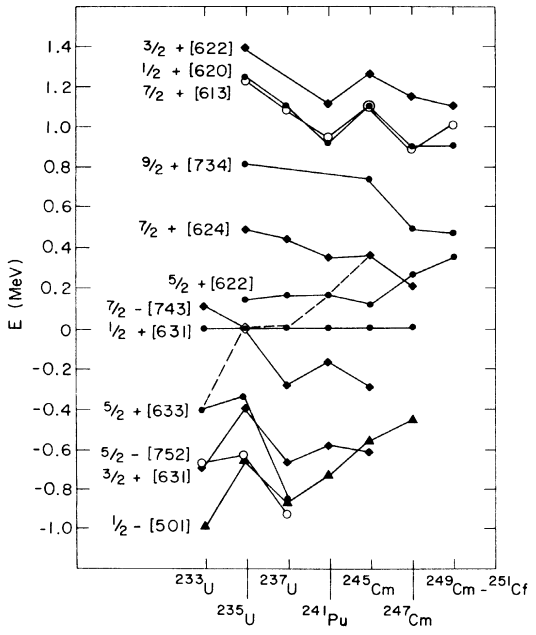

FIG. 2. Experimentally observed energy spacings of seniority-one odd-neutron nuclides. The dashed line indicates the ground state.

tween particle and hole excitation for convenience in these plots. For the odd-neutron nuclides ^{233}U–^{247}Cm, the energies are plotted relative to the orbital $\frac{1}{2}+[631]$; for 153 isotones, to the orbital $\frac{1}{2}+[620]$. All proton energies are plotted relative to the orbital $\frac{5}{2}+[642]$. By and large,

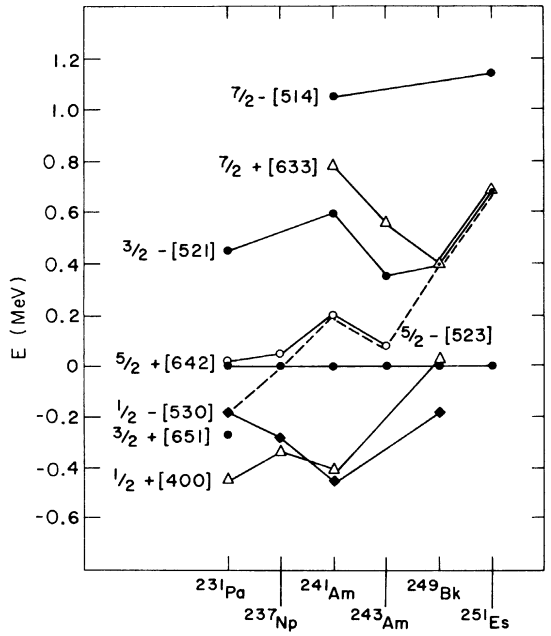

FIG. 3. Experimentally observed energy spacings of seniority-one odd-proton nuclides.

the spacings are similar for other nuclides having the same values of Z or N.

In Fig. 4, we have plotted the extracted neutron single particle energies obtained from the data of Fig. 2, using the DDDI. There are some noteworthy features in the extracted level spacings. We first note the comparatively reasonable behavior of the orbital $\frac{7}{2}-[743]$ relative to the orbital $\frac{1}{2}+[631]$. In Fig. 5, we display the extracted spacings for these orbitals using constant pairing matrix elements. In ^{241}Pu, there remains something of a problem with either set of matrix elements. There is a possibility of distinguishing between the two sets of matrix elements here. With constant pairing matrix elements, one calculates that in ^{234}U, the orbitals $\frac{7}{2}-[743]$ and $\frac{1}{2}+[631]$ have approximately equal occupation probabilities; $\langle N_{7/2-}\rangle = 0.17$, $\langle N_{1/2+}\rangle = 0.19$. With the DDDI matrix elements, the situation is quite different; we get $\langle N_{7/2-}\rangle = 0.21$, $\langle N_{1/2+}\rangle = 0.11$. Here the bracketed N is a ground state occupation probability. In ^{236}U, it is somewhat harder to distinguish between the two matrix element sets as the energy of the $\frac{7}{2}-$ orbital is shifting so much relative to the $\frac{1}{2}+$ orbital, using constant matrix elements for the analysis of ^{235}U and ^{237}U. For

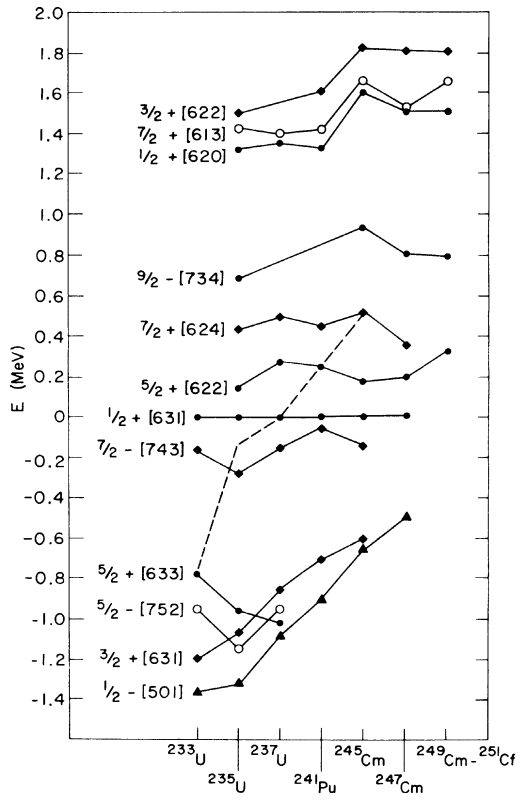

FIG. 4. Extracted neutron single particle spectra using DDDI matrix elements.

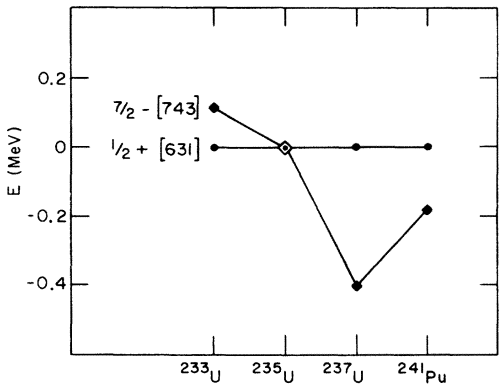

FIG. 5. Extracted energy spacing between $\frac{7}{2}-[743]$ and $\frac{1}{2}+[631]$ using constant pairing matrix elements.

the DDDI matrix elements, we get $\langle N_{1/2+}\rangle = 0.28$ and $\langle N_{7/2-}\rangle = 0.63$ in ^{236}U. Hopefully, the occupation probabilities in ^{234}U and ^{236}U can be accurately determined in single neutron transfer experiments. The improvement in the regularity of the $\frac{7}{2}-$ to $\frac{1}{2}+$ level spacing with the DDDI matrix elements is due to the larger than average pairing matrix elements associated with the $j_{15/2}$ orbitals.

The other $j_{15/2}$ orbital that is seen in many actinides is the $\frac{9}{2}-[734]$ orbital. In all of the discussion that follows, we have taken into account the ~100 keV energy shifts in the $\frac{9}{2}-[734]$ and $\frac{5}{2}+[622]$ orbitals that are due to coupling[13] with the 2^- phonon in ^{247}Cm and ^{249}Cm. These effects are also included in Fig. 4. In Fig. 6, we have plotted the extracted single particle levels in ^{245}Cm, ^{247}Cm, and ^{249}Cm obtained with constant pairing matrix elements. The apparent shift of the $\frac{9}{2}-[734]$ orbital in Fig. 6 is particularly striking and rather difficult to explain. With the DDDI matrix elements, there is no problem. We also note that the improvements in the behavior of the $\frac{5}{2}+[622]$ orbital are due to the fact that it has weaker than average pairing matrix elements as well as being due to the strong $\frac{9}{2}-[734]$ matrix elements.

There remain several features of the extracted neutron single particle spectrum that are not well explained by the DDDI matrix elements. These features are also not explained in the context of constant pairing matrix elements. The first such feature is the large increase in excitation energy of the particle orbitals $\frac{1}{2}+[620]$, $\frac{7}{2}+[613]$, and $\frac{3}{2}+[622]$ on going from ^{241}Pu to ^{245}Cm. This shift cannot be easily understood in terms of a deformation change of the single particle potential. Also, it is hard to maintain that there has been a sudden shift in energy of the excited orbitals due to phonon coupling effects, because the whole group of orbitals is shifted almost equally. A second difficulty is the large change in the extracted energy of the orbital $\frac{3}{2}+[631]$ with mass number. The behavior cannot be understood on the basis of reasonable changes in the deformation parameters. It might be of interest to examine the properties of this state in heavier nuclei, such as ^{241}Pu.

A most interesting open problem in the actinides is the nature of the low-lying 0^+ excited states. It is particularly difficult to understand why the 0^+ excited state in ^{234}U is at so low an excitation energy, using constant pairing matrix elements and the single particle spectrum extracted with them. The extracted single particle spectra of ^{233}U and ^{235}U displayed in Fig. 4 suggest the possibility of a low-lying pairing vibration in ^{234}U. We have calculated the energy of the 0^+ pairing excited state in ^{234}U, using the DDDI matrix elements and previously discussed methods.[14] We get a 0^+ excited state at 1350 keV, in extremely poor agreement with the experimental[15] value of 810 keV. If we assume that this 0^+ state is a proton pairing excitation, we get an even higher excitation energy. Clearly, the DDDI matrix elements do not explain the 0^+ excited state although they contain the prolate-oblate effect which has often been invoked to explain these states.

In Fig. 7, we have plotted the extracted proton single particle energy spacings obtained with the

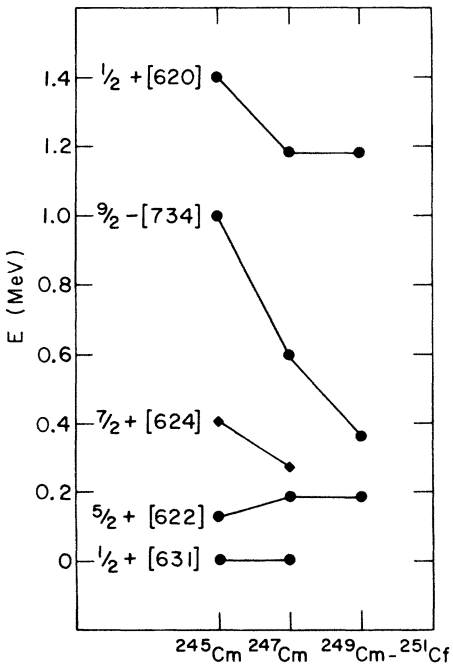

FIG. 6. Extracted neutron single particle spectra using constant matrix elements.

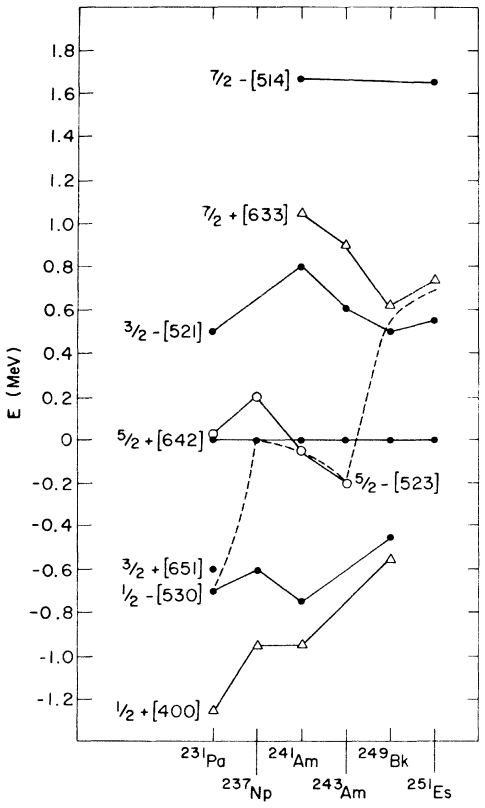

FIG. 7. Extracted proton single particle spectra using DDDI matrix elements.

DDDI matrix elements. There are two aspects of the proton level spacings that are nicely accounted for by the DDDI matrix elements and are difficult to understand with constant matrix elements. The first of these difficulties is the extracted single particle level spacings that one obtains for ^{231}Pa using constant pairing matrix elements. This difficulty is illustrated in Fig. 8, which is taken from a previous analysis[16] of proton states in the actinides. In Fig. 8, we see that the extracted level spacings, using constant pairing matrix elements, are much smaller than the spacings one calculates with a Woods-Saxon single particle potential. A glance at Fig. 7 shows that the extracted single particle level spacings obtained with the DDDI matrix elements are in substantially better agreement with the predictions of the single particle model calculations. We find that the deformation parameters $\epsilon_2 = 0.18$ and $\epsilon_4 = -0.03$ give a rather good description of the extracted level spacings obtained with the DDDI matrix elements. Our deformation parameters are introduced as shape deformations of the potential via the substitution

$$r^2 \to r^2\{\sin^2\theta\,\mathcal{E}^{2\epsilon_{2/3}} + \cos^2\theta\,\mathcal{E}^{-4\epsilon_{2/3}} + (2\pi)^{1/2}[\epsilon_4 Y_4^0(\theta) + \epsilon_6 Y_6^0(\theta)]\} \quad (16)$$

and correspond very closely to those of Nilsson for the quadrupole and hexadecapole deformations.

The second feature that we would like to explain in terms of the DDDI matrix elements is somewhat less obvious. In Fig. 3, we see the change in energy spacing of the orbitals $\frac{5}{2}-[523]$ and $\frac{5}{2}+[642]$ in the isotopes ^{237}Np, ^{241}Am, and ^{243}Am. We note that this spacing is about the same in ^{239}Np as it is in ^{237}Np and it gets smaller in ^{245}Am (~28 keV). This picture is not changed when the extracted level spacings are determined with constant pairing matrix elements. It is easiest to interpret these changes in the spacing by changing the ϵ_4 deformation parameter in ^{241}Am, making it more negative than it is in either ^{237}Np or ^{243}Am. Although this is not at all impossible, it seems somewhat implausible that the ϵ_4 deformation parameter should be fluctuating in this way. Further, the deformations inferred for neighboring even nuclides from Coulomb excitation experiments[17] indicate that the ϵ_4 deformation parameter is continuously becoming more positive with increasing mass. The direct determination of deformation parameters is, however, still a rather unsettled[18] subject. The DDDI matrix elements provide a more plausible picture of the ϵ_4 deformation parameter here. In Fig. 7, we see that the $\frac{5}{2}-[523]$ orbital is dropping continuously relative to the $\frac{5}{2}+[624]$ orbital in this region. This is consistent with a monotonic increase of the ϵ_4 deformation parameter with increasing mass.

Using the single particle spectra extracted with

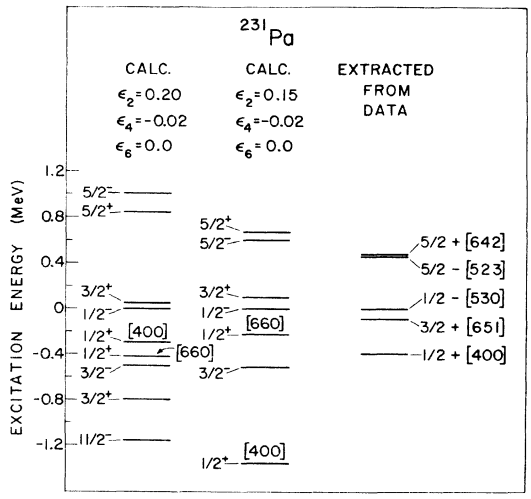

FIG. 8. Extracted proton single particle spectrum in ^{231}Pa using constant matrix elements.

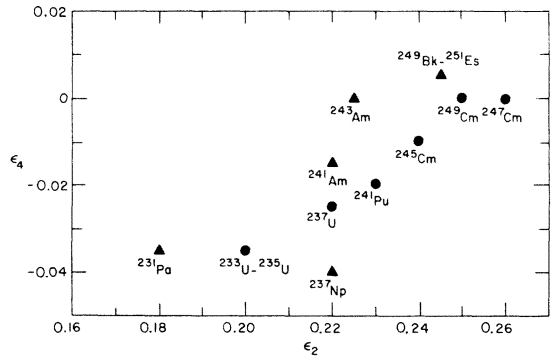

FIG. 9. Quadrupole and hexadecapole deformations of actinide nuclides.

the DDDI matrix elements, we have inferred deformation parameters ϵ_2 and ϵ_4 for the actinide nuclides. We note the approximate relations[19] between ϵ and β parameters

$$\beta_2 \approx 1.06\epsilon_2 + 0.20\epsilon_2^2 - 1.8\epsilon_2\epsilon_4, \tag{17a}$$

$$\beta_4 \approx -1.18\epsilon_4 + 0.27\epsilon_2^2 - 1.2\epsilon_2\epsilon_4. \tag{17b}$$

On the whole the agreement between extracted spectra and the single particle spectra calculated with a deformed Woods-Saxon potential is good for the levels near the ground state; better than the agreement that one obtains using constant pairing matrix elements. The deformation parameters that we infer are displayed in Fig. 9. The deformations that we obtain in this way for odd-proton and odd-neutron nuclides are in rough agreement with each other. Both sets of nuclides show the same trends in the deformation parameters as a function of mass. We found also that for ^{249}Bk, ^{251}Es, and ^{249}Cm the value of $\epsilon_6 \approx 0.01$ is suggested by the extracted level spacings. The sudden change in the inferred value of ϵ_4 for the (mass ~240) odd-proton nuclides comes from the changes in extracted spacing of the $\frac{5}{2}-[523]$ and $\frac{5}{2}+[642]$ orbitals. If the differences in the average pairing matrix elements associated with these orbitals were slightly smaller, the change in the ϵ_4 deformation parameter would also be smaller. The overall trends that we infer from the level spacings are consistent with the other determinations of the deformation parameters.[17,18] They are not in good agreement with the deformations that we infer using constant pairing matrix elements. This is not surprising in view of the differences in the extracted spectra.

IV. CONCLUSIONS AND SUMMARY

The main results of this work are contained in Tables I and II and in the extracted spectra of Figs. 4 and 7. Making comparisons with the results obtained with constant pairing matrix elements, we find that the DDDI matrix elements do provide a comparatively good description of actinide spectra. Several features of actinide spectra that are rather mysterious in the context of constant pairing matrix elements are nicely explained with the DDDI matrix elements. Although we have not discussed simple δ function matrix elements in this paper, we note that they also give an inferior description of the actinides in comparison with the DDDI matrix elements.

It remains to be seen how smoothly the parameters of the DDDI vary as a function of mass. It also remains to be seen to what extent the picture of the actinides that we have obtained with the DDDI pairing matrix elements will be distorted by the inclusion of particle-hole terms in the residual interaction.

It is a pleasure to acknowledge helpful conversations with I. Ahmad, A. Friedman, W. Ogle, and J. O. Rasmussen on this work.

*Based on work performed under the auspices of the U.S. Energy Research and Development Administration.

[1]I. M. Green and S. A. Moszkowski, Phys. Rev. 139B, B790 (1965).
[2]G. L. Struble and J. D. Immele, Phys. Rev. C (to be published).
[3]A. B. Migdal, *Theory of Finite Fermi Systems and Applications to Atomic Nuclei* (Interscience, New York, 1967).
[4]P. Ring and J. Speth, Nucl. Phys. A235, 315 (1974).
[5]T. H. R. Skyrme, Phil. Mag. 1, 1043 (1956); Nucl. Phys. 9, 615 (1959).
[6]Ph. Quentin, J. Phys. (Paris) 34, C4-101 (1973).
[7]R. R. Chasman, Phys. Rev. C 3, 1803 (1971).
[8]J. W. Ehlers and S. A. Moszkowski, Phys. Rev. C 6, 217 (1972).
[9]D. Kolb, R. Y. Cusson, and H. W. Schmitt, Phys. Rev. C 10, 1529 (1974).
[10]J. D. Immele and G. L. Struble, Nuovo Cimento Lett. 7, 41 (1973).
[11]R. R. Chasman, Phys. Rev. C 5, 29 (1972).
[12]I. Ahmad, R. R. Chasman, J. R. Erskine, and A. M. Friedman (unpublished).
[13]S. W. Yates, R. R. Chasman, A. M. Friedman, I. Ahmad, and K. Katori, Phys. Rev. C 12, 442 (1975).
[14]R. R. Chasman, Nucl. Phys. A119, 476 (1968).
[15]C. M. Lederer, J. M. Hollander, and I. Perlman, *Table of Isotopes* (Wiley, New York, 1967).
[16]J. R. Erskine, G. Kyle, R. R. Chasman, and A. M. Friedman, Phys. Rev. C 11, 561 (1975).
[17]C. E. Bemis, Jr., F. K. McGowan, J. L. C. Ford, Jr., W. T. Milner, P. H. Stelson, and R. L. Robinson, Phys. Rev. C 8, 1466 (1973).
[18]J. P. Davidson, D. A. Close, and J. J. Malanify, Phys. Rev. Lett. 32, 337 (1974).
[19]F. A. Gareev, S. P. Ivanova, and V. V. Paskevitch, JINR Report No. E4-4704, Dubna, 1969 (unpublished).